Journal of Power Sources 508 (2021) 230328

Contents lists available at ScienceDirect

Journal of Power Sources

journal homepage: www.elsevier.com/locate/jpowsour

# Techno-economic and Environmental Comparison of Internal Combustion Engines and Solid Oxide Fuel Cells for Ship Applications

Lukas Kistner, Fritjof L. Schubert, Christine Minke *, Astrid Bensmann, Richard Hanke-Rauschenbach

*Institute of Electric Power Systems, Electric Energy Storage Systems Section, Leibniz Universität Hannover, Germany*

## GRAPHICAL ABSTRACT

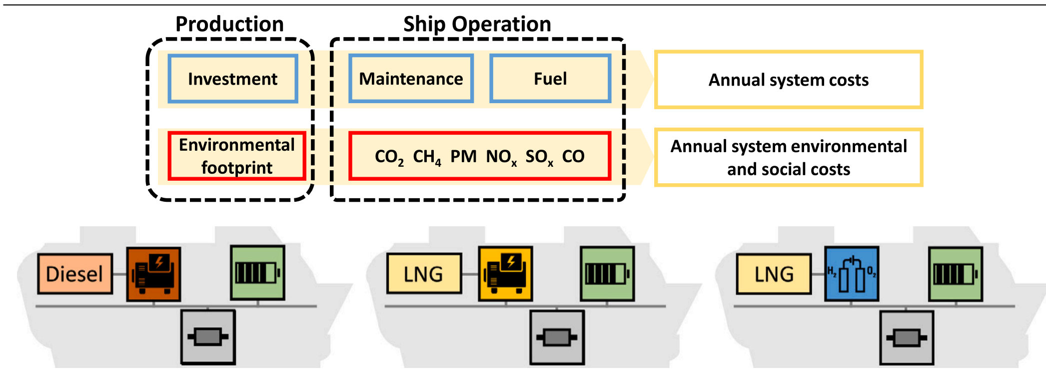


## HIGHLIGHTS

- Direct comparison of shipboard diesel/gas engines and solid oxide fuel cells.
- Design optimization of hybrid ship systems for equitable comparison.
- Simulation of capital, operating, and environmental costs with dynamic models.
- Forecast with technology development and the use of synthetic fuel in 2050.

## ARTICLE INFO

*Keywords:*
Ship energy systems
Solid oxide fuel cells
Energy system design optimization
Environmental assessment
Decarbonization of the shipping sector

## ABSTRACT

In order to quantify the economic and environmental impact of technology selection in ship power systems, four different battery-supported hybrid configurations including diesel and gas combustion engines, as well as natural gas fueled solid oxide fuel cells (SOFCs) are modeled and analyzed. The investigations include component investments, maintenance and operational costs, as well as the components' and fuels' carbon footprints, operational greenhouse gases and other relevant emissions. Dynamic energy system models are used to derive economically optimal system designs for an appropriate technology comparison in a cruise ship case study.

The assessment is conducted for a cruise ship case study with technology parameters for the near future and 2050. Results indicate that the auxiliary power system based on diesel combustion is inferior both economically and environmentally compared to SOFCs or gas combustion engines. While latter are the most cost efficient, SOFC application provides an environmental improvement without the need for a new fuel such as hydrogen. In a final outlook for the year 2050, SOFCs economically overtake gas combustion engines on the condition that their investment costs decrease and synthetic fuels are introduced to the market as a low emission solution.

* Corresponding author.
*E-mail address:* minke@ifes.uni-hannover.de (C. Minke).

https://doi.org/10.1016/j.jpowsour.2021.230328
Received 28 May 2021; Received in revised form 13 July 2021; Accepted 28 July 2021
Available online 10 August 2021

**List of Symbols**

| | |
|---|---|
| $A$ | Annuity factor (1/a) |
| $C_{E,B}$ | Battery energy capacity (kWh) |
| $C_{m,B}$ | Energy density (Wh/kg) |
| $c^{a}_{gen}$ | Maintenance cost factor (1/a) |
| $D_c$ | Control parameter (–) |
| $F_B$ | Battery state of energy (–) |
| $F^{high}_B$ | Desired highest state of energy (–) |
| $F^{low}_B$ | Desired lowest state of energy (–) |
| $g_{gen}$ | Generator cost exponent (–) |
| $h^{LHV}$ | Lower heating value (MJ/kg) |
| $j$ | Interest rate (–) |
| $k$ | ICE on/off control (–) |
| $M$ | Molar mass (kg/mol) |
| $m^{a}_{gen}$ | Annual operating mass in/output (kg) |
| $m^{eq,a,prod}_{CO2}$ | Component $CO_2$ eq. footprint (kg) |
| $m_{gen,fuel}$ | Passage consumed fuel mass (kg) |
| $m^{a}_{gen,fuel}$ | Annually consumed fuel mass (kg) |
| $\dot{m}^{rel}$ | Specific operating mass in/output (g/kWh) |
| $N_{SOFC}$ | Number of SOFC modules (–) |
| $P$ | Power (kW) |
| $P^{r}$ | Rated power (kW) |
| $P^{max}_{B,cha}$ | Battery max. charge power (kW) |
| $P^{max}_{B,dis}$ | Battery max. disch. power (kW) |
| $P^{high}_{CE}$ | Desired highest ICE output (kW) |
| $P^{low}_{CE}$ | Desired lowest ICE output (kW) |
| $P^{r}_{CE,l}$ | Large ICE rated power (kW) |
| $P^{r}_{CE,s}$ | Small ICE rated power (kW) |
| $P^{r}_{SOFC,mod}$ | SOFC module rated power (kW) |
| $P^{min}_{SOFC}$ | SOFC minimum power output (kW) |
| $\dot{P}^{max}_{SOFC,spec}$ | max. spec. SOFC power gradient (1/min) |
| $P_{set}$ | Desired power (kW) |
| $P_{m,gen}$ | Generator power density (W/kg) |
| $p^{a}$ | Annual costs (€/a) |
| $p^{inv}_{B}$ | Battery investment costs (€/kWh) |
| $p^{a}_{CO2,P}$ | Annual predicted $CO_2$ emission costs (€/a) |
| $p^{a}_{CO2,S}$ | Annual social $CO_2$ emission costs (€/a) |
| $p_{fuel}$ | Fuel price (€/MWh) |
| $p^{inv}_{gen}$ | Generator investment costs (€/kW) |
| $p^{a}_{gen,I}$ | Generator investment annuity (€/a) |
| $p^{a}_{gen,M}$ | Annual maintenance costs (€/a) |
| $p_{LNG,fee}$ | Extra LNG port fee (€/MWh) |
| $t$ | Time (s) |
| $t^{a}$ | Annual operating time (h) |
| $t^{e}$ | Passage time (h) |
| $t_L$ | Component lifetime (a) |
| $V$ | Volume ($m^3$) |
| $\zeta$ | $GWP_{100}$ factor ($kg_{CO2}$/kg) |
| $\eta$ | Energy efficiency (–) |
| $\kappa^{eq}_{CO2}$ | Mass specific $CO_2$ eq. footprint ($kg_{CO2}$/kg) |
| $\lambda^{eq}_{CO2}$ | Power specific $CO_2$ eq. footprint ($kg_{CO2}$/W) |
| $\xi$ | Mass fraction ($kg/kg_{fuel}$) |
| $\rho$ | Density ($kg/m^3$) |
| $\varphi^{high}$ | Relative desired highest ICE output (–) |
| $\varphi^{low}$ | Relative desired lowest ICE output (–) |
| $\chi$ | Specific (social) emission costs (€/kg) |
| $\chi_{CO2,P}$ | Predicted $CO_2$ emission fee (€/kg) |
| $\chi_{CO2,S}$ | Social $CO_2$ emission costs (€/kg) |

**List of Component and Fuel Indices**

| | |
|---|---|
| B | Battery |
| DCE | Diesel combustion engine |
| SOFC | Solid oxide fuel cells |
| fuel | VLSFO/LNG |
| GCE | Gas combustion engine |
| gen | Power generator |
| CE | Combustion engine (DCE/GCE) |
| L | Load |
| LNG | Liquefied natural gas |
| SNG | Substitute natural gas |
| st | SOFC stack |
| VLSFO | Very low sulfur fuel oil |

**List of Emission Indices**

| | |
|---|---|
| BC | Black carbon |
| carb | BC/$CH_4$ |
| $CH_4$ | Methane |
| CO | Carbon monoxide |
| $CO_2$ | Carbon dioxide |
| LE | CO/$NO_x$/$SO_x$ |
| $NO_x$ | Nitrogen oxides |
| $SO_x$ | Sulfur oxides |

## 1. Introduction

In the face of the International Maritime Organisation's (IMO) climate protection targets that come into force in 2050 [1], the marine traffic sector debates the possible substitution of conventional power generators with fuel cells. To contribute a factual assessment to this discussion, the subject of this paper is the appropriate, direct comparison of state-of-the-art ship diesel combustion engines (DCE), gas combustion engines (GCE), and solid oxide fuel cell (SOFC) systems. This system comparison is important at the present time, as many in the maritime industry remain skeptical about early stage investments in new technologies and focus on maintaining the status quo.

The IMO states that a ship's defined Energy Efficiency Design Index must be reduced by 50% starting in 2050 compared to a 2008 reference. However, the IMO does not actively plan to fine remaining emissions or to determine legally binding reduction milestones prior to 2050. Moreover, there exists little national political pressure on the deep sea shipping sector. Nevertheless, emission reduction approaches must not be delayed until 2050 because marine traffic constitutes a significant share of anthropogenic emissions with and without global warming potential [2,3]. While more and more large scale joint projects launch to investigate different fuel cell technologies and fuel combinations [4,5], criticism from maritime industry participants persists based on three ideas: (1) fuel cell systems imply too high capital costs, (2) early investing in the wrong technology leads to a major disadvantage for the shipowner, and (3) hydrogen lacks in availability and volumetric energy density. To remedy the weak spots of hydrogen, several system approaches focus on the usage of ammonia, methanol or even conventional fuels like diesel or liquefied natural gas (LNG) [6]. The latter's availability can be assumed, as LNG is bunkered in 24 of the largest 25 ports and in 76% of all ports worldwide [7].

In the literature, there already exist several combined economic and environmental investigations concerning fuel cells with non-hydrogen fueling for ship operation. For example, the authors of [9] conducted

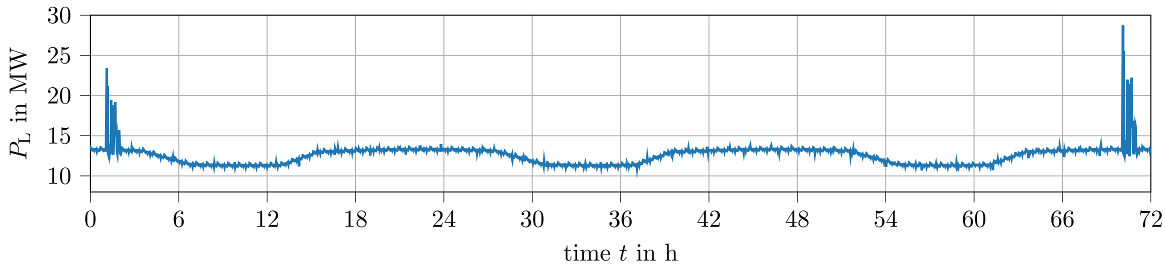


**Fig. 1.** 72 h passage with day–night rhythm hotel load and two harbor maneuvers [8].

a life cycle analysis of a diesel-fed molten carbonate fuel cell system in 2006. The authors integrated three different ship operation modes for a defined energy system. For the SOFC technology, the authors of [10] characterized the environmental effects of a methanol-based operation with a special focus on the fuel production. In the operation phase, their work builds upon fixed fuel cell efficiency. Recently in [11], the SOFC systems' energy, cost, and emission reduction potentials are analyzed on the basis of daily load profiles, but again with static fuel consumption. In [12], diesel combustion was compared to several fuel cell technologies and fuel combinations economically and environmentally. Unlike the investigated combustion engine, fuel cell systems were supported by an energy storage system in this analysis. The assessment is based on predefined component designs, constant efficiencies and staggered load scenarios.

As stated, none of these approaches consider the highly operation-point-dependent efficiencies and emissions of the power generation technologies, instead choosing averaged estimations or even full load specifications. However, ship load profiles tend to have a very fluctuating characteristic. In this paper, dynamic energy system models are presented, which take into account the nonlinear behavior of DCE, GCE, and SOFC components with a uniform level of detail. The simulation results include direct system costs, volume, all relevant emissions and their social costs. Also, no prefixed component sizes are assumed, to avoid distortion of the results. Instead, an objective assessment of the power source technologies is ensured by comparing cost-optimal designed systems. The option of system hybridization with a battery unit is also included as a cost and emission reduction measure for every considered system [13].

The results of these investigations aim to refute the ship industry's long-standing prejudices surrounding fuel cells with the example of an SOFC system running on LNG. Even if the capital costs of SOFCs are larger than the costs of internal combustion engines (ICE), higher SOFC energy efficiency will lead to the reduction of a ship's fuel costs that represent a large expense for ship owners [14]. While the operation with natural gas will not lead to emission neutrality, byproducts of a combustion like nitrogen oxides, carbon monoxide and particulate matter would be eliminated in addition to the reduction of carbon dioxide. The quantification and valuation of realistic fuel consumption and emissions will be essential for the conducted system comparison beyond pure economic aspects. As it is uncertain if states or state associations will price pollutants of the shipping industry in the future, their effect's social costs will be consulted to properly evaluate emission reduction.

This paper is organized as follows: Section 2 offers an overview of the case study ship and the energy system configurations considered for optimization. In Section 3, techno-economic and environmental equation systems are presented for components and fuels. Section 4 covers the system cost optimization results and the follow-up environmental emissions' evaluation. In Section 5, optimization results are revised for the use of synthetic fuels and technology advances in 2050.

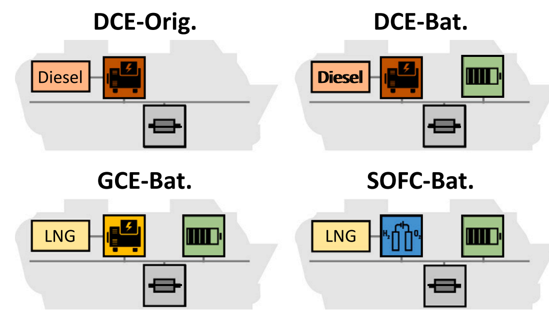


**Fig. 2.** Considered system configurations for the case study.

## 2. Case study, component configurations, system optimization, and controls

### 2.1. Case study

The conducted case study is based on a 330 m long cruise ship built for 4100 passengers and a crew of 1700. The investigated electrical load profile of a 72 h passage from [8] presents hotel load, maneuver, and operation energy consumption of more than 900 MWh but excludes propulsion power. For the dynamic simulation, the load profile was superimposed with two different records for sea and maneuver operation with an increment size of one second. The profile with day–night rhythm, typical for hotel operation, and two harbor thruster maneuvers is depicted in Fig. 1. It is assumed that this kind of open sea operation occurs at least 300 days per year and is suspended only for daytime mooring at tourist destinations and maintenance days.

In a model-based simulation, four energy system configurations with different power sources are designed to comply with the load demand. The following configurations are summarized in Fig. 2:

**DCE-Orig.** is the original design case that replicates the real system configuration. Three small and three large auxiliary engines combine for more than 59 MW rated power. The original design is not used for a direct technology evaluation, but should signal that the comparison of prefixed and optimized systems distorts the results significantly.

**DCE-Bat.** is built from three large and three small diesel engines, but with cost-optimal sizes. For a fair assessment, the optimization approach includes battery support to form a hybrid configuration.

**GCE-Bat.** is composed of three large and three small optimal sized natural gas combustion engines with an additional battery.

**SOFC-Bat.** is built of a variable number of SOFC modules with a natural gas reformer and a rated power of 300 kW each. Like the other configurations, the system is supported by a battery unit. The size of the SOFC modules roughly represents the aspired single system size for market introduction.

### 2.2. System design optimization

To determine the competitiveness of the SOFC technology in an open market, an energy system comparison is conducted for economically optimized designs, whereas environmental social costs are neglected. The problem formulation to minimize the annual total system costs is as follows:

$$\begin{aligned} \underset{P^{\mathrm{r}}_{\mathrm{gen},i}, C_{\mathrm{E,B}}, F_{\mathrm{B}}(t_0), D_{\mathrm{c}}}{\text{minimize}} \quad & p^{\mathrm{a}}_{\mathrm{gen}} + p^{\mathrm{a}}_{\mathrm{B}} + p^{\mathrm{a}}_{\mathrm{fuel}} \\ \text{subject to} \quad & 0 = P_{\mathrm{gen}}(t) - P_{\mathrm{L}}(t) - P_{\mathrm{B}}(t)\,\forall t\,, \\ & F_{\mathrm{B}}(t_0) \le F_{\mathrm{B}}(t_{\mathrm{end}})\,, \\ & \text{Eqs. (2) – (23)}. \end{aligned} \tag{1}$$

Total annual system costs are composed of annual generator costs $p^{\mathrm{a}}_{\mathrm{gen}}$, annual battery costs $p^{\mathrm{a}}_{\mathrm{B}}$, and annual fuel expenses $p^{\mathrm{a}}_{\mathrm{fuel}}$. The first ship design degree of freedom is the rated power of the generator $P^{\mathrm{r}}_{\mathrm{gen}}$. The index "gen" is a placeholder for either DCE, GCE or SOFC and the index $i$ takes into account the discussed modularity possibilities of the case study that have already been stated in Section 2.1. For the combustion genset, three large and three small auxiliary engines are simulated:

$$P^{\mathrm{r}}_{\mathrm{CE}} = 3\,P^{\mathrm{r}}_{\mathrm{CE,l}} + 3\,P^{\mathrm{r}}_{\mathrm{CE,s}}\,, \tag{2}$$

where the index CE is a placeholder for either DCE or GCE, $P^{\mathrm{r}}_{\mathrm{CE,l}}$ is the rated power of one large combustion engine, and $P^{\mathrm{r}}_{\mathrm{CE,s}}$ is the rated power of one small engine. The modular fuel cell system rated power can be calculated with

$$\begin{aligned} P^{\mathrm{r}}_{\mathrm{SOFC}} &= P^{\mathrm{r}}_{\mathrm{SOFC,mod}} \cdot N_{\mathrm{SOFC}} \\ &= 300\,\mathrm{kW} \cdot N_{\mathrm{SOFC}}\,, \end{aligned} \tag{3}$$

where $P^{\mathrm{r}}_{\mathrm{SOFC,mod}}$ is the rated power of one module and $N_{\mathrm{SOFC}}$ is the number of SOFC modules. Further degrees of freedom are the energy capacity of the battery $C_{\mathrm{E,B}}$, its state of energy at the beginning of the passage $F_{\mathrm{B}}(t_0)$ and the placeholder $D_{\mathrm{c}}$, which represents several control parameters adjusted by the optimization algorithm. The first constraint denotes the mandatory power supply requirement and states, that the generator power $P_{\mathrm{gen}}$ must equal the load demand $P_{\mathrm{L}}$ and the battery charge demand $P_{\mathrm{B}}$, as no excess energy or load shedding is permitted. An additional cyclic boundary for the battery indicates that its state of energy $F_{\mathrm{B}}$ at beginning of operation must not exceed the value at end of operation to guarantee operational functionality past the simulation time frame. The Eqs. (2)–(23) present component limitations and control strategies, which must be complied with, as well as the economic equation system to calculate the annual system costs. Their formulation is given in Sections 3.1 and 3.2, respectively.

All of the following models and control strategies were created in the object-orientated programming language *Modelica* with help of the *OpenModelica 1.17.0* editor *OMEdit* [15]. Simulations and optimizations were executed in *Python* with the Differential Evolution algorithm and the interface *OMPython*.

## 3. Techno-economic and environmental models

In this section, the equation systems for component models, system controls, direct system costs and the environmental impact are introduced. The overall scope of the analysis is depicted in Fig. 3. The key economic elements (top, blue) include the component investment costs for the preparation segment, as well as maintenance and fuel expenses for the ship operation segment. The latter are influenced by the ship's load profile and resulting system responses (green). The system behavior is also taken into account for the environmental assessment (bottom, red). Analogous to the economic analysis, components and fuels are investigated for the preparation and operation phases. Total systems costs and emissions are then evaluated for the technology comparison (yellow).

### 3.1. Components' physical models and control strategies

The control strategies' objectives are derived from the characteristic component behavior, which is also included in the analysis with the help of system level physical models. For the SOFC and the battery, dynamic models have been parameterized in [16]. Here, the outlined technology-neutral storage model was chosen in combination with the degradation approach from [17]. As the combustion engines do not show relevant dynamic limitations, their physical behavior is represented by their operation-specific fuel consumption, which is discussed in Section 3.2.

In hybrid systems, a power management strategy must specify desired power outputs for each component, as one's operation goal is not necessarily the compensation of the consumption demand. In addition to ensuring the power balance, which was already stated in the constraints of Eq. (1), these set values follow a defined strategy, which in this case includes battery peak load shaving operation. Apart from this aspect, the system controls for ICE and SOFC based systems are described separately, as they focus on different issues.

**Case 1: Combustion engines and battery** — The first power management strategy is used for the two battery-supported combustion engine configurations "DCE-Bat." and "GCE-Bat.". The strategy includes three control parameters adjusted by the optimization algorithm: $F^{\mathrm{low}}_{\mathrm{B}}$ symbols a critically low battery state of energy, $\varphi^{\mathrm{low}}$ and $\varphi^{\mathrm{high}}$ are specific lower and higher limitations for the desired ICE operating window. Derived limitation values for a given engine design are calculated as:

$$P^{\mathrm{low}}_{\mathrm{CE}} = \varphi^{\mathrm{low}} \cdot P^{\mathrm{r}}_{\mathrm{CE}}\,, \tag{4}$$

$$P^{\mathrm{high}}_{\mathrm{CE}} = \varphi^{\mathrm{high}} \cdot P^{\mathrm{r}}_{\mathrm{CE}}\,. \tag{5}$$

In addition to reducing the required ICE rated power, the battery application improves fuel consumption by keeping the ICE operating point in the predefined window for as long as possible. The battery set value specifies charging with the help of a larger ICE power output when its state of energy is critical ($F_{\mathrm{B}} < F^{\mathrm{low}}_{\mathrm{B}}$), peak load shaving, or part load avoidance for the ICE:

$$P_{\mathrm{B,set}} = \begin{cases} P_{\mathrm{CE}} - P_{\mathrm{L}} & \text{if} \quad F_{\mathrm{B}} < F^{\mathrm{low}}_{\mathrm{B}} \\ P^{\mathrm{high}}_{\mathrm{CE}} - P_{\mathrm{L}} & \text{elseif} \quad P_{\mathrm{L}} > P^{\mathrm{high}}_{\mathrm{CE}} \\ P^{\mathrm{low}}_{\mathrm{CE}} - P_{\mathrm{L}} & \text{elseif} \quad P_{\mathrm{L}} < P^{\mathrm{low}}_{\mathrm{CE}} \\ 0 & \text{else}\,. \end{cases} \tag{6}$$

The set value is controlled to not violate the following limitations or is otherwise reduced according to [16]:

$$0\% \le F_{\mathrm{B}} \le 100\%\,, \tag{7}$$

$$P^{\mathrm{max}}_{\mathrm{B,dis}} \le P_{\mathrm{B}} \le P^{\mathrm{max}}_{\mathrm{B,cha}}\,, \tag{8}$$

where $P_{\mathrm{B,dis}}$ is the maximum discharge power and $P_{\mathrm{B,cha}}$ is the maximum allowed charge power, which are both dependent on the battery size.

Next, the combustion engines' set value is introduced. Analogous to the battery's desired power, the ICE output power should increase to charge the storage if the battery's state of energy is too low. Else, the ICEs work in a load-following mode. If possible, they stay in the desired operation range:

$$P_{\mathrm{CE,set}} = \begin{cases} P_{\mathrm{L}} + P^{\mathrm{max}}_{\mathrm{B,cha}} & \text{if} \quad F_{\mathrm{B}} < F^{\mathrm{low}}_{\mathrm{B}} \\ P_{\mathrm{L}} + P_{\mathrm{B}} & \text{else}\,. \end{cases} \tag{9}$$

As the summed up set power value for the combustion engines is not provided by one engine, but by six smaller units, they are further controlled with a on/off switch logic, that is presented in the following.

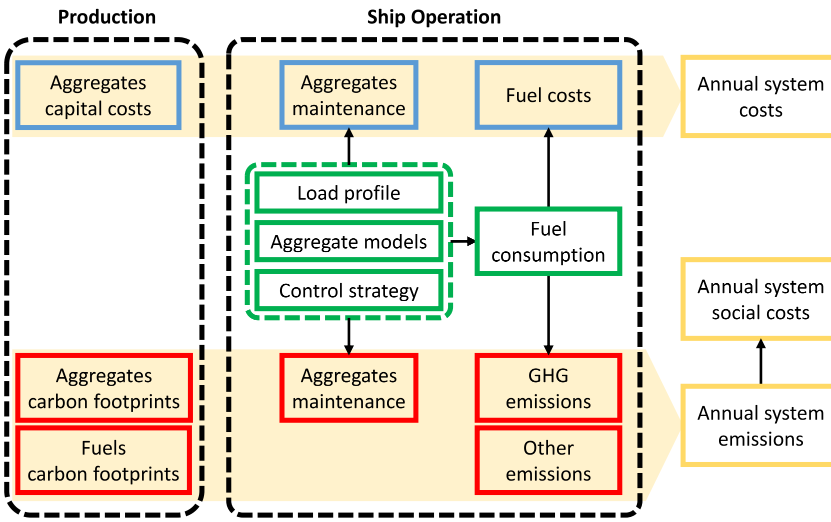


**Fig. 3.** Scope of the conducted economic (blue) and environmental (red) assessments, influenced by system behavior (green). (For interpretation of the references to color in this figure legend, the reader is referred to the web version of this article.)

This approach was also used for the "DCE-Orig." case. Since the engines exhibit a better efficiency in high part load operation, as few units as possible are operating at one time. While doing so, the switched on units' rated power needs to be adequate for the desired total power:

$$\begin{aligned} &\underset{\vec{k}}{\text{minimize}} && \sum_{j=1}^{6} k_j \cdot P^{\mathrm{r}}_{\mathrm{CE},j} \\ &\text{subject to} && P_{\mathrm{CE,set}} \le \sum_{j=1}^{6} k_j \cdot P^{\mathrm{r}}_{\mathrm{CE},j} \\ &&& k_j = \{0,1\} \end{aligned} \tag{10}$$

where $k_j$ is an on/off switch for each of the six auxiliary engines. The total power is equally distributed across all engines, considering their rated power as the upper output limit:

$$P_{\mathrm{CE}} = \sum_{j=1}^{6} \min\left( P_{\mathrm{CE,set}} \cdot \frac{k_j \cdot P^{\mathrm{r}}_{\mathrm{CE},j}}{\sum_{g=1}^{6} k_g \cdot P^{\mathrm{r}}_{\mathrm{CE},g}}, P^{\mathrm{r}}_{\mathrm{CE},j} \right). \tag{11}$$

Note that start-up times and minimum runtimes of ship ICEs are omitted to simplify the model. However, the given load profile grants smooth operation transitions most of the time during this passage.

**Case 2: SOFCs and battery** — The second power management strategy was created for the "SOFC-Bat." configuration. The SOFC system has two limitations that must be addressed by the control strategy in order to ensure proper system behavior. First, during operation, the systems must not fall below a minimum power output 50% part load to maintain proper fluid behavior and avoid cooling below a required temperature [16]:

$$P^{\min}_{\mathrm{SOFC}} = 0.5 \cdot P^{\mathrm{r}}_{\mathrm{SOFC}} \le P_{\mathrm{SOFC}} \le P^{\mathrm{r}}_{\mathrm{SOFC}}. \tag{12}$$

Second, a maximum power gradient must be complied with due to thermo-mechanical tensions:

$$\begin{aligned} \left| \frac{\mathrm{d}P_{\mathrm{SOFC}}}{\mathrm{d}t} \right| &\le \dot{P}^{\max}_{\mathrm{SOFC,spec}} \cdot P^{\mathrm{r}}_{\mathrm{SOFC}} \\ &\le 0.1\,\mathrm{min}^{-1} \cdot P^{\mathrm{r}}_{\mathrm{SOFC}}. \end{aligned} \tag{13}$$

In addition to peak load shaving, the battery usage allows the coverage of the fluctuating load profile, which would not be given with the application of an SOFC system with power gradient limitations. Therefore, it is advisable to keep the battery ready for use. This is done by controlling its state of energy and keeping it within a desired corridor between the limits $F^{\mathrm{low}}_{\mathrm{B}}$ and $F^{\mathrm{high}}_{\mathrm{B}}$. Both parameters are adjusted by the optimization algorithm. The battery set value always aims to compensate the difference between fuel cell power and load demand to assure the power balance:

$$P_{\mathrm{B,set}} = P_{\mathrm{SOFC}} - P_{\mathrm{L}}. \tag{14}$$

If the battery's state of energy leaves the desired range, the fuel cell system adapts in order to counteract the critical state and minimizes or maximizes the output. Otherwise, fuel cells should try to follow the load while complying with the gradient limitations, to reduce the required battery power:

$$P_{\mathrm{SOFC,set}} = \begin{cases} P^{\mathrm{r}}_{\mathrm{SOFC}} & \text{if} \quad F_{\mathrm{B}} < F^{\mathrm{low}}_{\mathrm{B}} \\ 0.5\, P^{\mathrm{r}}_{\mathrm{SOFC}} & \text{if} \quad F_{\mathrm{B}} > F^{\mathrm{high}}_{\mathrm{B}} \\ P_{\mathrm{L}} & \text{else}. \end{cases} \tag{15}$$

### 3.2. Economic model

The economic model is separated into component and fuel costs.

#### 3.2.1. Component costs and maintenance

Diesel combustion engines are by far the most commonly used power technology and had a market share of 98% in 2018 [18]. On the other hand, LNG based system numbers are growing by up to 40% per year, and while not many ships are retrofitted with gas engines, more than 10% of newly built deep-sea orders are LNG-fueled [19]. Both options prove to be relevant for the market and are therefore modeled and analyzed. For auxiliary DCEs in the investigated dimensions, 4-stroke engines with comparably higher friction losses are selected, because 2-strokes with lower rotation speed and a larger power output are designed mainly for propulsion [20,21]. For auxiliary GCEs, lean burn spark ignited engines are considered over dual fuel engines for rated powers from 0.5 to 8 MW due to their lower fuel slip [22]. The investigated SOFC system contains an external steam reforming module constructed for natural gas conversion to improve fuel conversion rate and dynamic limitations.

The annual power generator costs consist of investment and maintenance cost:

$$\begin{aligned} p^{\mathrm{a}}_{\mathrm{gen}} &= p^{\mathrm{a}}_{\mathrm{gen,I}} + p^{\mathrm{a}}_{\mathrm{gen,M}} \\ &= p^{\mathrm{inv}}_{\mathrm{gen}} \cdot \left(P^{\mathrm{r}}_{\mathrm{gen}}\right)^{g_{\mathrm{gen}}} \cdot \left(A_{\mathrm{gen}} + c^{\mathrm{a}}_{\mathrm{gen}}\right) \end{aligned} \tag{16}$$

where $p^{\mathrm{a}}_{\mathrm{gen,I}}$ is the component's annuity, $p^{\mathrm{inv}}_{\mathrm{gen}}$ is the specific capital investment, $p^{\mathrm{a}}_{\mathrm{gen,M}}$ are the maintenance costs based on a cost factor $c^{\mathrm{a}}_{\mathrm{gen}}$ and

$$A = \frac{(1+j)^{t_{\mathrm{L}}} \cdot j}{(1+j)^{t_{\mathrm{L}}} - 1} \tag{17}$$

**Table 1**
Solid oxide fuel cell (SOFC), LFP battery (B), diesel combustion engine (DCE) and gas combustion engine (GCE) parameters for cost and volume calculation ("manuf." parameters are obtained from manufacturers and include own market analyses).

| Parameter | | Value | Ref. |
|---|---|---|---|
| Spec. invest. DCE | $p^{inv}_{DCE}$ | 251.19 €/kW$^{1.1}$ | [24] |
| Spec. invest. GCE | $p^{inv}_{GCE}$ | 301.43 €/kW$^{1.1}$ | [24,25] |
| Spec. invest. SOFC | $p^{inv}_{SOFC}$ | 2000 €/kW | [26] |
| Spec. invest. Bat | $p^{inv}_{B}$ | 800 €/kWh | manuf. |
| Cost exp. ICE | $g_{CE}$ | 1.1 | [24] |
| Cost exp. SOFC | $g_{SOFC}$ | 1 | – |
| Mainten. ICE | $c^a$ | 0.0045 a$^{-1}$ | [28] |
| Mainten. SOFC | $c^a_{SOFC}$ | 0.04 a$^{-1}$ | [29,30] |
| Life time gen. | $t_{L,gen}$ | 20 a | [4] |
| Life time bat. | $t_{L,B}$ | Variable | [17] |
| Density ICE | $\rho_{CE}$ | 648.43 kg/m$^3$ | [31] |
| Power den. ICE | $P_{m,ICE}$ | 57.143 W/kg | [9] |
| Density SOFC | $\rho_{SOFC}$ | 450 kg/m$^3$ | manuf. |
| Power den. SOFC | $P_{m,FC}$ | 14.82 W/kg | manuf. |
| Density Bat | $\rho_B$ | 387.8 kg/m$^3$ | manuf. |
| Energy den. Bat | $C_{m,B}$ | 44.29 Wh/kg | manuf. |
| Interest rate | $j$ | 0.035 | – |

is the component's annuity factor based on its lifetime $t_L$ and the assumed interest rate $j$. ICE investment costs do not increase linearly with their rated power and are modeled with an exponential fit function according to [23] and a growth factor $g_{gen}$ derived from state-of-the-art prices [24]. Investment costs for GCEs also imply exponential dependence, but are 20%–24% higher than for DCEs today [24,25]. SOFC costs are modeled to behave proportionally to the rated power. An achievable price goal for a timely market introduction is assumed [26].

As SOFCs cannot keep up with ICEs' volumetric power density [27], the investigation also includes a rough size requirement comparison. The generators' volumes are calculated with their density $\rho_{gen}$ and power density $P_{m,gen}$:

$$V_{gen} = \frac{P^r_{gen}}{P_{m,gen} \cdot \rho_{gen}} . \tag{18}$$

Cost and volume of the selected Lithium Iron Phosphate (LFP) batteries are calculated analogously, but all specific parameters refer to energy capacity instead of power:

$$p^a_B = p^{inv}_B \cdot C_{E,B} \cdot A_B , \tag{19}$$

$$V_B = \frac{C_{E,B}}{C_{m,B} \cdot \rho_B} . \tag{20}$$

All parameters required for the cost and volume calculations are listed in Table 1.

### 3.2.2. Marine fuels and consumption calculation

In 2019, marine heavy fuel oils with a sulfur amount up to 3.5% had a market share of 73%, followed by marine gas oils [18]. Since 2020, heavy fuel oil use is only permitted in combination with an exhaust gas cleaning system also called scrubber [32]. An alternative to installing a scrubber is the use of very low sulfur fuel oils (VLSFO) with a sulfur content of up to 0.5%. While this allows operation in open sea, special zones with a 0.1% limitation already exist [33]. VLSFO was chosen for the diesel system simulations, as it is predicted to heavily increase in relevance in the next years.

The tightening of sulfur limitations and the greenhouse gas emission reduction targets also result in growing interest in LNG as ship fuel. LNG contains close to no sulfur and is also less expensive than diesel fuels [34,35]. Standard natural gas consists of 87%–96% methane. During its combustion, approximately 25% less carbon dioxide is emitted per energy unit compared to heavy fuel oils [22,36].

Fuel consumption rates of DCEs, GCEs and SOFCs heavily influence the economic evaluation of the energy systems. Specific fuel

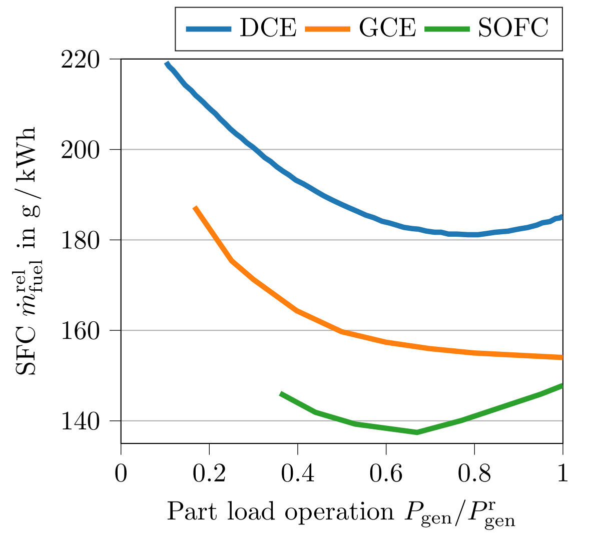


**Fig. 4.** Specific fuel consumption (SFC) curves for DCE [37], GCE [36], and SOFC (data obtained from manufacturers).

**Table 2**
Fuel parameters for cost and volume calculation (LHV: lower heating value).

| Parameter | | Value | Ref. |
|---|---|---|---|
| Price VLSFO | $p_{VLSFO}$ | 0.553 €/kg | [38] |
| Price LNG | $p_{LNG}$ | 14.04 €/MWh | [35] |
| Port fee VLSFO | $p_{VLSFO,fee}$ | Included | [35] |
| Port fee LNG | $p_{LNG,fee}$ | 5 €/MWh | [35,39] |
| Density VLSFO | $\rho_{VLSFO}$ | 940 kg/m$^3$ | [40] |
| Density LNG | $\rho_{LNG}$ | 450 kg/m$^3$ | [41] |
| LHV LNG | $h^{LHV}_{LNG}$ | 45.1 MJ/kg | [42] |

consumption (SFC) mass flows $\dot{m}^{rel}_{gen,fuel}$ have been chosen to represent the components' operating point dependent efficiencies. State-of-the-art curves with regard to engine type and size are shown in Fig. 4. Both ICE technologies show a decreasing efficiency for lower part load operating points, while the SOFCs maintain their efficiency advantage in their limited operation corridor.

For the conducted investigation, first the fuel consumption for the analyzed passage is calculated:

$$m_{gen,fuel} = \int^{t_e} \dot{m}^{rel}_{gen,fuel}\left(P_{gen}\right) \cdot P_{gen}(t)\, dt \tag{21}$$

where the index "fuel" is a placeholder for either VLSFO or LNG and $t_e$ is the time of the passage. The emerging fuel costs are extrapolated to the annual operating time $t^a$:

$$p^a_{fuel} = \frac{t^a}{t^e} \cdot m_{gen,fuel} \cdot \left(p_{fuel} + p_{fuel,fee}\right) , \tag{22}$$

where $p_{fuel}$ is the fuel price including potential port fees. While a ship's fuel tank is not designed to last for only one passage, the consumed fuel volume

$$V_{fuel} = \frac{m_{gen,fuel}}{\rho_{fuel}} \tag{23}$$

can be used as an indicator for possible differences between the diesel and LNG systems. Fuel parameters are listed in Table 2.

### 3.3. Environmental assessment

The most relevant emissions coming from ship traffic are sulfur oxides ($SO_x$), nitrogen oxides ($NO_x$), carbon monoxide (CO), particulate matter including black carbon (BC), methane ($CH_4$), and carbon dioxide ($CO_2$) [36,43]. For this study, emission valuation is separated into the categories "effects with global warming potential" and "negative local

**Table 3**
$CO_2$-equivalent emissions for supply of components and fuels.

| Parameter | | Value | Ref. |
|---|---|---|---|
| DCE | $\kappa^{eq}_{DCE,CO_2}$ | 4.843 $kg_{CO_2,eq}/kg$ | [46] |
| GCE | $\kappa^{eq}_{GCE,CO_2}$ | 4.843 $kg_{CO_2,eq}/kg$ | [46] |
| SOFC sys. | $\lambda^{eq}_{SOFC,CO2}$ | 0.82 $kg_{CO_2,eq}/W$ | [47] |
| SOFC stack | $\lambda^{eq}_{SOFC-st,CO_2}$ | 0.114 $kg_{CO_2,eq}/W$ | [45] |
| Battery | $\kappa^{eq}_{B,CO_2}$ | 7.88 $kg_{CO_2,eq}/kg$ | [48] |
| VLSFO | $\kappa^{eq}_{VLSFO,CO_2}$ | 0.5907 $kg_{CO_2,eq}/kg$ | [49] |
| LNG | $\kappa^{eq}_{LNG,CO_2}$ | 0.8344 $kg_{CO_2,eq}/kg$ | [49] |

effects". Component production, fuel provision, and ship operation are quantified separately.

*3.3.1. Emissions with global warming potential*

**Production of components and fuels** — For a comprehensive environmental analysis, not only the emissions occurring during operation, but also the raw material extraction and production emissions are considered. Here, databases often feature mass specific carbon dioxide equivalent emissions $\kappa^{eq}$ or power specific emissions $\lambda^{eq}$. For the comparison of different emissions, a reference period of 100 years ($GWP_{100}$) is used [44]. The total calculated emissions for each component are evenly distributed for the annual emission comparison:

$$m^{eq,a,prod}_{CE,CO2} = \frac{1}{t_{L,ICE}} \cdot \frac{P^r_{CE}}{P_{m,ICE}} \cdot \kappa^{eq}_{CE,CO2}, \tag{24}$$

$$m^{eq,a,prod}_{SOFC,CO2} = \frac{1}{t_{L,FC}} \cdot P^r_{SOFC} \cdot \left(\lambda^{eq}_{SOFC,CO2} - \lambda^{eq}_{SOFC-st,CO2}\right) + \dots \\ \frac{1}{t_{L,FC,st}} \cdot P^r_{SOFC} \cdot \lambda^{eq}_{SOFC-st,CO2}, \tag{25}$$

$$m^{eq,a,prod}_{B,CO2} = \frac{1}{t_{L,B}} \cdot \frac{C^r_{E,B}}{C_{m,B}} \cdot \kappa^{eq}_{B,CO2}, \tag{26}$$

$$m^{eq,a,prod}_{fuel,CO2} = m^a_{fuel,CO2} \cdot \kappa^{eq}_{fuel,CO2}. \tag{27}$$

Note that in Eq. (25), SOFC system and cell stacks are treated separately and $t_{L,FC,st}$ is the stack lifetime assumed in [45]. All carbon footprints are listed in Table 3.

**Operation** — Recently, the IMO estimated that the marine industry accounted for 2.89% of anthropogenic greenhouse gases in 2018 [2]. While this share falls behind other transportation sectors, it still presents an expedient reduction potential. For the analysis, the emitted carbon dioxide mass during ship operation is calculated with the combustion stoichiometry and considers other carbon-based emissions:

$$m^a_{gen,CO2} = \left(m^a_{gen,fuel} - m^a_{gen,CH4}\right) \cdot \frac{M_{CO2}}{M_C} \cdot \dots \\ \left(\xi_{C,fuel} - m^a_{gen,BC} - \frac{M_{CO}}{M_C} \cdot m^a_{gen,CO}\right), \tag{28}$$

where $m^a_{gen,CH4}$, $m^a_{gen,BC}$, $m^a_{gen,CO}$ are the annual methane, black carbon, and carbon monoxide emissions, and $M_C$, $M_{CO}$, $M_{CO2}$ are the substances' molar masses.

In spark ignited GCEs, not all natural gas molecules take part in the combustion reaction. Instead, a fraction of the hydrocarbons leaves the engine unburnt [51]. The rate of this effect called methane slip increases for lower part load operating points [22]. The assumed dependency is depicted in Fig. 5(a). Neither for SOFCs nor for DCEs does a similar effect occur.

Black carbon is the most relevant component of particulate matter regarding global warming [52]. It is a result of incomplete fuel burning

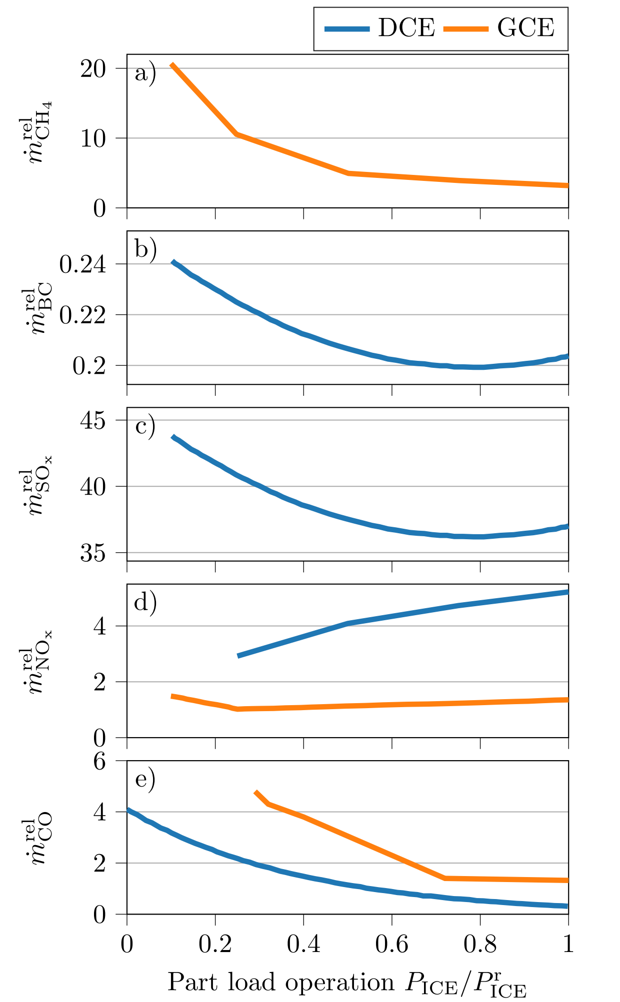


**Fig. 5.** Operation-point-dependent $CH_4$ [22], BC [50], $SO_x$ [33], $NO_x$ [22,43], and CO emissions [37,51] of DCE and GCE in g/kWh (electrical power).

and its production rate is not highly related to the operating point [53]. For VLSFO, the BC production rate is outlined in [50] and depicted in Fig. 5(b). For LNG engines, BC emissions have been proven not to be relevant [51].

In analogy to the system's fuel consumption in Eq. (21), annual emissions are extrapolated from the integrated masses of the investigated passage:

$$m^a_{CE,carb} = \frac{t^a}{t^e} \int^{t_e} \dot{m}^{rel}_{CE,carb}\left(P_{CE}\right) \cdot P_{CE}(t)\,dt, \tag{29}$$

where $\dot{m}^{rel}_{CE,carb}$ is the operation-dependent emitted mass, which is normalized on the generator power output and the index "carb" is a placeholder for BC and $CH_4$. The $CO_2$-equivalent effects of BC and $CH_4$ are calculated with

$$m^{eq,a}_{CE,CO2-carb} = \zeta_{carb} \cdot m^a_{CE,carb}, \tag{30}$$

where $\zeta_{carb}$ is the related $GWP_{100}$ factor listed in Table 4.

**Monetary valuation of emissions with global warming potential** — Today, it seems unlikely that all flag states will agree on worldwide uniform greenhouse gas emission fees in near future. While the European Parliament discusses $CO_2$ emission reduction targets of 40% by 2030, calls for a bill to tax maritime operation with 25 €/$t_{CO2}$ have been made. Alternatively, the ship industry could be included in the European Emissions Trading System with prices in the same price category [54]. As it is unsure if the laws apply for open sea traffic, and

**Table 4**
Fuel parameters, $GWP_{100}$, and emissions cost grading for the environmental investigation.

| Cost parameter | | Value | Ref. |
|---|---|---|---|
| VLSFO carb.. | $\xi_{C,VLSFO}$ | 85.44% | [43] |
| LNG carb. | $\xi_{C,LNG}$ | 75.68% | [41] |
| BC $GWP_{100}$ | $\zeta_{BC}$ | 680 $kg_{CO_2eq}/kg_{BC}$ | [57] |
| $CH_4$ $GWP_{100}$ | $\zeta_{CH4}$ | 30 $kg_{CO_2eq}/kg_{CH_4}$ | [58] |
| Social cost $SO_x$ | $\chi_{SO_x}$ | 10.72 €/$kg_{SO_x}$ | [59] |
| Social cost $NO_x$ | $\chi_{NO_x}$ | 9.29 €/$kg_{NO_x}$ | [59] |
| Social cost CO | $\chi_{CO}$ | 0.997 €/$kg_{CO}$ | [59] |
| Likely cost $CO_2$ | $\chi_{CO_2,P}$ | 25 €/$t_{CO_2eq}$ | [60] |
| Social cost $CO_2$ | $\chi_{CO_2,S}$ | 106.25 €/$t_{CO_2eq}$ | [56] |

aspects like pricing, emissions scope and life cycle considerations have not yet been negotiated, a fixed price for all greenhouse gases including production emissions is assumed for the investigations. It is calculated with

$$p^{a}_{CO2,P} = m^{a}_{CO2} \cdot \chi_{CO2,P}\,, \tag{31}$$

where $\chi_{CO2,P}$ is the predicted upcoming carbon dioxide emission fee. That being said, this price highly diverges from requested values in climate protection organizations and scientific articles. Here, many different values have been suggested [55], but social costs below 106,25 €/$t_{CO2}$ are estimated to be unrealistic [56]. Therefore, additional social costs have been calculated:

$$p^{a}_{CO2,S} = m^{a}_{CO2} \cdot \left(\chi_{CO2,S} - \chi_{CO2,P}\right) \tag{32}$$

where $\chi_{CO2,S}$ is the minimum socially acceptable carbon dioxide fee.

### *3.3.2. Emissions with primary negative local effects*

**Production of component and fuels** — The petrochemical and the steel industry are among the largest industrial emitters of nitrogen oxides, and oil refineries also produce an abundance of sulfur oxides [61,62]. However, this part of the assessment focuses on local emissions that affect the open sea and coastal ecosystem caused by marine traffic. Unlike the greenhouse gas emissions, adding up all emission sources distorts the analysis, as different environments cannot easily be compared to each other. Analyzing average effects of industry in different ecosystems is out of the paper's scope.

**Operation** — The ship industry produces 4%–9% of human sulfur oxides emissions, causing acidification of marine ecosystems and the reduction of their biodiversity [3]. Diesel fuels are the main sulfur source, whereas LNG contains only 3.5 ppm [63]. Relative sulfur oxide emissions for diesel combustion are depicted in Fig. 5(c). Like black carbon, they grow proportionally with the consumed fuel [33].

15% of the anthropogenic nitrogen oxides lead back to ship traffic [3]. Formation of tropospheric ozone, eutrophication of the waters, and generation of acid rain are directly relatable to these emissions [59,64,65]. In ICEs, the $NO_x$ production rates depend on oxygen supply and combustion temperature. Therefore, they do not share the trend of higher relative emissions for lower part load operations. Characteristic curves for diesel and gas combustion are presented in Fig. 5(d) [22,43].

While carbon monoxide (CO) is a respiratory poison in higher concentrations, long-term damages in an open environment are harder to determine [66].

Nevertheless, CO takes part in the formation of tropospheric ozone like nitrogen oxides. Characteristic emission curves for DCEs and GCEs are shown in Fig. 5(e) [37,51].

For the quantification of annual emissions, the operation-point-dependent normalized emission factors $\dot{m}^{rel}_{CE,LE}$ shown in Fig. 5 are, in turn, integrated over the investigated passage time and extrapolated over one year:

$$m^{a}_{CE,LE} = \frac{t^{a}}{t^{e}} \int^{t_e} \dot{m}^{rel}_{CE,LE}\left(P_{CE}\right) \cdot P_{CE}\left(t\right) \mathrm{d}t\,, \tag{33}$$

**Table 5**
Design comparison of real-life diesel system and cost-optimized hybrid systems.

| Designs in MW resp. MWh | | DCE-Orig. | DCE-Bat. | GCE-Bat. | SOFC-Bat. |
|---|---|---|---|---|---|
| Total gen. rated power | $P^{r}_{gen}$ | 59.49 | 16.338 | 15.88 | 14.1 |
| Rated power large | $P^{r,l}_{CE,j}$ | 11.33 | 5.095 | 3.053 | – |
| Rated power small | $P^{r,s}_{CE,j}$ | 8.5 | 0.351 | 2.241 | – |
| Battery rated capacity | $C_{E,B}$ | – | 2.373 | 2.459 | 3.601 |
| Battery discharge power | $P^{max}_{B,dis}$ | – | 16.94 | 17.55 | 25.71 |
| Total system power | | 59.49 | 33.278 | 33.43 | 39.81 |

where "LE" (local emissions) is a placeholder for $SO_x$, $NO_x$ or CO. Apart from the small sulfur content in LNG, the SOFC technology does not emit pollutants with negative local effects during operation.

**Monetary valuation of emissions with primary negative local effects** — Unlike greenhouse gases, locally active emissions should be rated with several environmental factors in mind. These include the type and sensitivity of the ecosystem, population density, and overall pollution burdens [3,59,67]. For the investigated case study, adequate cost factors $\chi_{LE}$ have been selected with regard to these influencing categories. The parameters are listed in Table 4. The valuation of considered emissions is calculated with:

$$p^{a}_{LE} = m^{a}_{LE} \cdot \chi_{LE}\,. \tag{34}$$

## 4. Results and discussion

In the following, the optimization results are presented. First, the direct cost optimized aggregate sizes are discussed. Subsequently, their resulting annual costs and aggregate volumes are compared to each other. Finally, the system emissions are listed and evaluated. To underline the possible distortion of comparing a prefixed system with a design that was exclusively adapted for the analyzed load profile, results for the original diesel layout are shown in each analysis. The "DCE-Bat." configuration was chosen as a benchmark.

### *4.1. Cost-optimal system configurations*

Key data of the four analyzed energy system designs are listed in Table 5. The original design stands out as the largest system with close to 60 MW installed power. Comparing it with the optimized and hybrid DCE system shows that the total installed power can be decreased by 45% and the generator power by 74% in this specific case. Most likely, the original design resulted from simultaneity factor calculation or estimations based on knowledge plus safety factors. It is already evident, that a fair technology comparison between the power generators could not have been made with only the original design case.

The cost optimized system configurations (last three columns in Table 5) show more similarities, but do not present identical total rated power outputs. While the genset of six combustion engines provides approximately the same power for DCEs and GCEs, the distribution between the small and large engines varies significantly. These minor differences can be explained with help of the components' behavior and cost parameters: the power distribution for DCE and GCE components differ because their specific fuel consumption diverges (cf. Fig. 4). Toreduce costs, the engine design aims for an optimal average energy efficiency without overdimensioning the components. While active, the DCE average relative operating point is 0.91 with a range 0.69 from to 1. The GCE average operating point is 0.957 with a range from 0.71 to 1. In addition to the design incentive of high energy efficiency, the aggregate investment costs also influence the design decision: as the GCE installation costs are higher than the DCE costs, slightly larger batteries are utilized for the maneuver peak load shaving.

The SOFC rated power is 12% smaller than the power of the two ICE technologies. In return, a disproportionately larger battery was chosen

**Table 6**
Annual component, fuel, and total system costs.

| Costs in mil. €/a | | DCE-Orig. | DCE-Bat. | GCE-Bat. | SOFC-Bat. |
|---|---|---|---|---|---|
| Generator | $p^{a}_{gen,I}$ | 2.643 | 0.668 | 0.742 | 1.984 |
| Maintenance | $p^{a}_{gen,M}$ | 0.169 | 0.043 | 0.047 | 1.128 |
| Battery | $p^{a}_{B}$ | – | 0.177 | 0.175 | 0.384 |
| Fuel | $p^{a}_{fuel}$ | 9.314 | 9.309 | 3.327 | 3.112 |
| Total annual costs | | 12.126 | 10.197 | 4.291 | 6.608 |
| Savings to DCE-Bat. | | −18.9% | – | 57.9% | 35.2% |

**Table 7**
Cost-optimized system components' sizes.

| Sizes in m$^3$ | | DCE-Orig. | DCE-Bat. | GCE-Bat. | SOFC-Bat. |
|---|---|---|---|---|---|
| Generator | $V_{gen}$ | 1606 | 441 | 429 | 2115 |
| Battery | $V_{B}$ | – | 113 | 117 | 172 |
| Fuel | $V_{fuel}$ | 176 | 175 | 311 | 291 |
| Total volume | | 1782 | 729 | 857 | 2578 |
| Rel. increase to DCE-Bat. | | 144% | – | 17.5% | 253.6% |

for support. The SOFC average specific operating point is 0.89 with a range from 0.73 to 1. Here, the high fuel cell system investment costs prevent a design that leads to lower, more advantageous average operating points around 0.66.

The discussed designs result in annual system costs summarized in Table 6. It can be seen that fuel costs are by far the largest annual investments for all systems. Installing a battery on the other hand is not costly compared to its numerous benefits, even if the aggregate has a comparably small lifetime. A cost optimization for the DCEs decreases the aggregate cost by installing a peak load shaving battery and foregoing possible redundancy factors. Fuel consumption cannot be reduced significantly. The gas engine system is the most profitable solution despite GCE's larger capital investment, because LNG prices are below VLSFO. In comparison, the SOFC is disadvantaged by the even higher aggregate investment costs, which cannot be compensated totally with energy efficiency. Nevertheless, the SOFC saves 35% annual costs compared to the optimized hybrid diesel system, proving to be economically more than reasonable.

Of course, the price trends of the two different fuels influence this assessment considerably. But even in more extreme price ratios, the results do not change qualitatively, as diesel and gas prices tend to interact strongly [35].

### 4.2. Energy system volume

As the SOFCs' volumetric power density is much smaller than the power density of an ICE, controlling the overall system volume is important when assessing the practicability of the fuel cell system. For this, design optimized system aggregate volumes are listed in Table 7. It can be seen that the SOFC system has a volume nearly five times the size of the cost optimized combustion engines. In this straightforward comparison, the DCE system wins due to the high volumetric energy density of diesel fuel.

On the other hand, for a holistic consideration, maintenance space, installation flexibility, realistic tank volume or other peripheral components like fuel inflow, cooling, exhaust pipes, required scrubbers and even maintenance crew cabins should also be investigated. Additionally, the modular SOFC installation grants system redundancy much more easily than six combustion engines. Furthermore, the derived system volume, mass and required installation area could be priced based on the type of ship to include the space requirement in the optimization function. These investigations are out of this paper's scope, but should be included in future economic research. Until then, the bottom line of this volume comparison is that the SOFC system's size is a drawback, but not an insurmountable obstacle in terms of practicability.

**Table 8**
System annual $CO_2$-equivalent emissions with emissions for battery and generators split equally among lifetime.

| $CO_2$-eq. in kt/a | | DCE-Orig. | DCE-Bat. | GCE-Bat. | SOFC-Bat. |
|---|---|---|---|---|---|
| Gen. $CO_2$-eq. | $m^{eq,a,prod}_{gen,CO_2}$ | 0.252 | 0.069 | 0.067 | 0.882 |
| Bat. $CO_2$-eq. | $m^{eq,a,prod}_{B,CO_2}$ | – | 0.0247 | 0.024 | 0.058 |
| Fuel $CO_2$-eq. | $m^{eq,a,prod}_{fuel,CO_2}$ | 10.152 | 10.07 | 11.646 | 10.853 |
| Operat. $CO_2$ | $m^{a}_{gen,CO_2}$ | 63.95 | 63.99 | 37.662 | 35.927 |
| Operat. $CH_4$ | $m^{a}_{GCE,CH_4}$ | 0 | 0 | 0.297 | 0 |
| Operat. BC | $m^{a}_{DCE,BC}$ | $18.1\cdot10^{-3}$ | $18.08\cdot10^{-3}$ | 0 | 0 |
| Total $CO_2$-eq. emissions | | 74.102 | 74.066 | 58.218 | 47.716 |
| Savings to DCE-Bat. | | −0.05% | – | 21.4% | 35.6% |

**Table 9**
System annual operational emissions with negative local effects.

| Exhaust in t/a | | DCE-Orig. | DCE-Bat. | GCE-Bat. | SOFC-Bat. |
|---|---|---|---|---|---|
| Operat. CO | $m^{a}_{gen,CO}$ | 51.592 | 45.083 | 120.431 | 0 |
| Savings to DCE-Bat. | | −14.4% | – | −167.1% | 100% |
| Operat. $NO_x$ | $m^{a}_{gen,NO_x}$ | 431.964 | 441.192 | 121.26 | 0 |
| Savings to DCE-Bat. | | 2.1% | – | 72.5% | 100% |
| Operat. $SO_x$ | $m^{a}_{gen,SOx}$ | 32.869 | 32.854 | 0.194 | 0.181 |
| Savings to DCE-Bat. | | −0.05% | – | 99.4% | 99.5% |

### 4.3. Environmental assessment

For the greenhouse gases, single emission sources and the total annual $CO_2$-equivalent masses are listed in Table 8. Operational emissions have the highest impact on the overall generation, followed by the emissions coming from fuel production. The consideration of components' production does not meaningfully change the outcome of the comparison, even though the SOFC emissions are one order of magnitude greater than ICE emissions. Despite the methane slip, the GCE system saves one fifth of the DCE annual greenhouse gases, but emits 18% more than the fossil fuel SOFC approach. The SOFC has the lowest impact on global warming due to its higher energy efficiency and the absence of methane slip or black carbon generation.

For an initial comparison of the natural gas driven systems, specific $CO_2$ avoidance costs of 220 €/$t_{CO2eq}$ can be predicted for the SOFC technology. While this seems to be relatively high compared to assumptions of 110 €/$t_{CO2eq}$ [56] or 68–119 €/$t_{CO2eq}$ [68], literature results most often involve diesel engines as a base case. In this case, since the DCE system approach is both environmentally, and economically inferior to the SOFC system approach, no specific $CO_2$ avoidance costs can be calculated.

The positive environmental effects of fuel cell usage will increase with the consideration of annual emissions with local effects, which are quantified in Table 9. A significant reduction of nitrogen and sulfur oxides is obtainable with LNG, regardless of the power technology. A countertrend is found only for the CO emissions, which increase by factor 2.7 for the GCE engines compared to the DCEs. For the SOFC system, nearly all emissions are cut to zero, except for the small percentage of sulfur found in LNG.

To visualize the impact of reducing emissions, their assumed social costs are added to the direct system costs in Fig. 6. Here, emissions with global warming potential are priced with the presumed upcoming fee and a socially appropriate pricing, respectively.

Social costs of both the original and the cost-optimized DCE system are significantly larger than costs caused by the LNG-based approaches. Even if an accommodating specific fuel consumption curve was assumed for the DCE, neither the direct costs nor the environmental impact seem to benefit a ship owner's goals. Independent from fuel price developments, newly built cruise ships should therefore not feature diesel engines. With the appointed costs of 25 €/$t_{CO2}$, the GCE

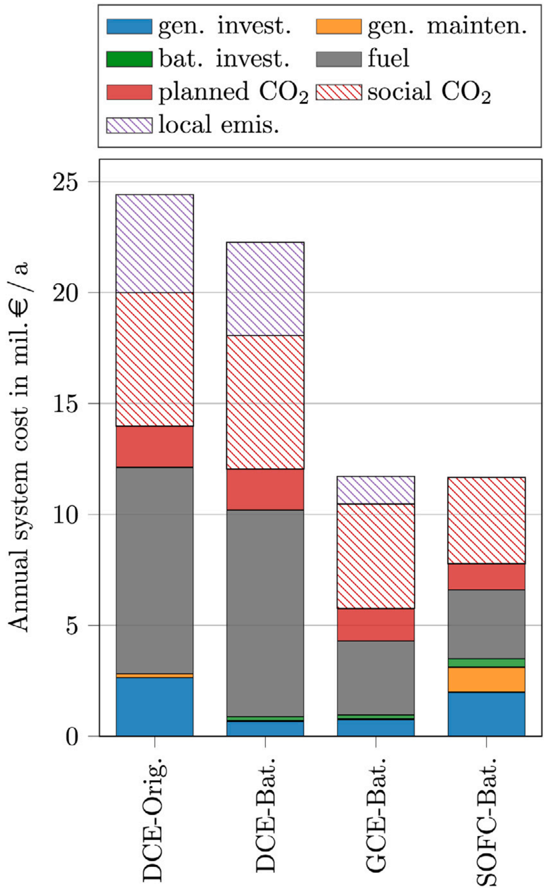


**Fig. 6.** Total system costs of the assessed configurations: annual power generator investment costs $p^{a}_{gen,I}$ (blue), annual generator maintenance costs $p^{a}_{gen,M}$ (orange), annual battery costs $p^{a}_{B}$ (green), annual fuel expenses $p^{a}_{fuel}$ (gray), GWP-relevant emissions valuated with discussed EU-price $p^{a}_{CO2,P}$ (red) and difference to estimated social value $p^{a}_{CO2,S}$ (red, shaded), as well as other social costs from local pollution $\sum p^{a}_{LE}$ (purple, shaded). (For interpretation of the references to color in this figure legend, the reader is referred to the web version of this article.)

still proves to be more cost effective than the SOFC. Today, when considering all social subsequent costs including non-greenhouse gases, the SOFC system barely surpasses the GCE in the ranking. Still, SOFCs will be an economically reasonable power source for ships in the near future.

Looking forward, technology advances and large scale aggregate production will very likely reduce the SOFC investment costs, which have proven to be the biggest disadvantage in direct economic comparisons. Also, a future shift towards synthetic fuels will further advantage the technology. Those predicted trends are discussed in the following section.

## 5. Further investigation: SOFC development and synthetic methane

Synthetic fuels are heavily discussed as a solution for emission reduction in the maritime industry. On the one hand, an environmentally friendlier yet still energy dense fuel is a promising approach to reach long-term objectives. On the other hand, fuels produced in power-to-x plants come with a harsh price increase, as their production is energy intensive and the steel, chemical and aviation industries also plan to use alternative energy carriers. Therefore, high energy system efficiencies on ships will become even more economically important in the future.

For this investigation, the natural gas-based system analyses have been revised with a substitute natural gas (SNG). SNG will likely not be available for ships on a large scale in the near future, but is inspected for long term strategies. Since the IMO will not regulate greenhouse gas emissions for the cruise ship industry until 2050 [1] and there are no economic incentives to purchase synthetic fuels today, estimated future prices and technology development are considered for the comparison. Unlike the GCEs, the SOFC technology is still improving in energy efficiency, investment costs, and degradation aspects. These improvements are implemented in the following analysis with the two studies "2050-GCE" and "2050-SOFC".

**Table 10**
SOFC and SNG parameters assumed for the year 2050.

| Parameter | | Value | Ref. |
|---|---|---|---|
| Cost SOFC | $p^{inv}_{SOFC}$ | 800 €/kW | [26] |
| Mainten. SOFC | $c^{a}_{SOFC}$ | 0.01536 $a^{-1}$ | [26] |
| SNG cost | $p_{SNG}$ | 60.95 €/MWh | [71] |
| SNG prod. em. | $\kappa^{eq}_{SNG,CO_2}$ | 0.237 $kg_{CO_2eq}/kg$ | [72] |
| $CH_4$ $GWP_{100}$ | $\zeta_{CH_4}$ | 28.25 $kg_{CO_2eq}/kg_{CH_4}$ | – |

### 5.1. System parameter revision

SOFC cost and lifetime adjustments are based on an estimation of 27 experts, who were interviewed in [26]. In the survey, capital investment savings of 70% and upwards for cells and systems are derived from technology performance, degree of market penetration, and manufacturing capability. Longer cell lifetimes and smaller stack costs also influence the maintenance cost factor of the SOFC. In 2050, stack costs take a 4% smaller fraction of the total capital costs than in 2020. The experts also address a 60% lower cell degradation rate. To account for the rising SOFC energy efficiency associated with the cell and plant development, the unit's specific fuel consumption is reduced. For this, the plant's electrical efficiency $\eta^{2050}_{SOFC}$ of 60% at full load is assumed to be reachable in the near future without including uncertain scientific breakthroughs on materials [69]. On that basis, the specific fuel consumption of the SOFC is evenly decreased independently of the operating point to reach the quoted value:

$$\dot{m}^{rel,2050}_{SOFC,SNG} = \frac{\eta_{SOFC}}{\eta^{2050}_{SOFC}} \cdot \dot{m}^{rel}_{SOFC,LNG} \approx 0.9 \cdot \dot{m}^{rel}_{SOFC,LNG} \,. \tag{35}$$

Another SOFC parameter that could be adjusted for this investigation is the aggregate's carbon footprint. However, as the first assessment displays its little influence on the overall outcome, the presumable emission reduction is neglected here.

The SNG price is dependent on production technology advances, electrical energy costs, and annual operating hours of the production plants. While current SNG prices are more then 20 times higher than prices for natural gas today [70], a scenario from [71] for cost estimation in 2050 indicates a price decrease. Here, the chosen costs are calculated for an assessed electrical energy price and for adequate plant operating time periods. SNG still has a carbon footprint from its production plants and electrical energy supply, but the ship operational $CO_2$ emissions are valuated at zero. Therefore, the accounting $GWP_{100}$ of methane $\zeta_{CH4}$ coming from SNG is also reduced by the carbon capture fraction. With hydrogen production and methanation energy demand from [72], exclusive use of solar power, and a carbon footprint estimated for electrical energy in 2050 [73], the gas production's emission parameters are adjusted for an optimistic outlook. The summarized alterations for the 2050 study are listed in Table 10.

### 5.2. Optimization results

The discussion of the optimization results follows the procedure from Section 4 but is reduced to the most important key aspects. As

**Table 11**
Cost optimal system design today with natural gas and in 2050 with SNG as fuel substitute.

| | | GCE-Bat. | 2050-GCE | SOFC-Bat. | 2050-SOFC |
|---|---|---|---|---|---|
| Total gen power in MW | $P^{r}_{gen}$ | 15.88 | 16.08 | 14.1 | 17.1 |
| Battery capacity in MWh | $C_{E,B}$ | 2.459 | 2.432 | 3.601 | 2.797 |

a major change in fuel cost will lead to new cost-optimal designs, the system optimization is repeated and results are listed in Table 11. Now that fuel efficiency is even more important, the cost-optimal configurations should lead to more efficient operating points. For the gas engine, less battery support and a slightly increased total generator power was chosen. The average relative operating point of 0.954 slightly undercuts previous values, but overall less part load operation and fewer permanently active engines lead to a decreased fuel consumption. More SOFC modules have been installed as they are now less expensive. This also leads to a more favorable average operating point of 0.735, and an operating range from 0.61 to 1. A higher number of SOFC modules also reduces the required battery capacity due to increasing dynamic response capability.

In a final step, economic and valued environmental results of the SNG-fueled future systems are compared to each other and to today's systems in Fig. 7. Under the assumption of SNG use in 2050, fuel expenses will have an even larger share of the total annual system costs. In return, the greenhouse gas emissions and relating fees decreased to a fraction of those for natural gas. Higher energy efficiency and future cost improvement of the SOFC technology lead to smaller system costs compared to gas engines in the future, even without including environmental aspects. Those results will be even more drastic, if greenhouse gas emissions are penalized with fees in 2050.

While present annual direct costs of the ship energy systems are lower than the SOFC system in 2050 thanks to low gas prices, the inclusion of emission valuation shifts the future SOFC system to the overall cheapest approach. Social costs of the 2050 SOFC system are 84% smaller than the 2050 GCE and 95% smaller than today's GCE system. These results certainly underline the importance of technology research and open-mindedness towards upcoming energy system solutions. If the SOFC technology development can meet the expectations, it will massively support the decarbonization and the reduction of other pollutants emitted by the shipping sector.

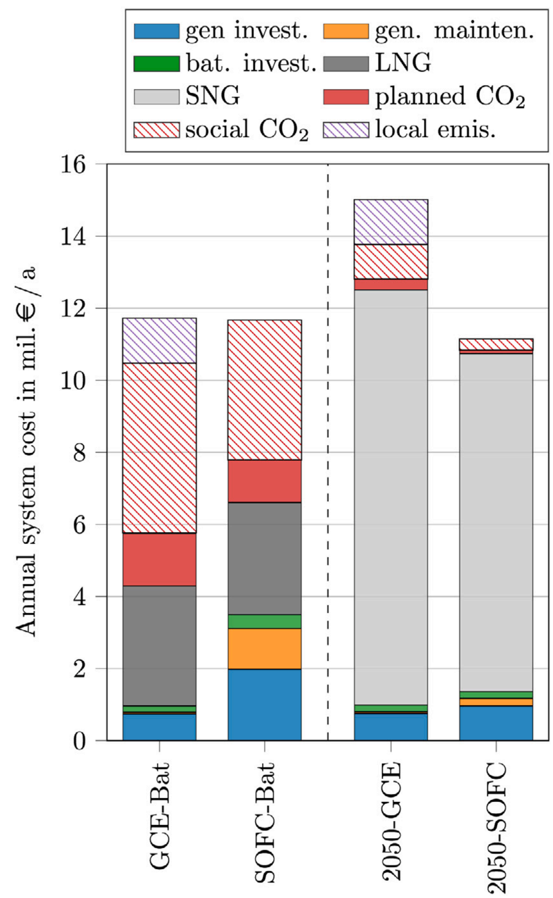


**Fig. 7.** Cost comparison of the systems running with natural gas (NG), when synthetic methane (SNG) is assumed to be an available fuel in 2050.

## 6. Conclusion

A comparison of optimized system designs enables a fair technology evaluation. If not all assessed systems are treated equally, results could be distorted significantly, as could be visualized with a ship's load profile and original energy system design. In this context, the same supporting system components such as energy storage units are assessed for all compared systems.

In our case study, the SOFC technology is viable for maritime applications from a purely economic perspective despite the larger capital and maintenance costs of the components. Today, annual system costs fall below those of conventional diesel combustion engines due to the high energy efficiency and the use of LNG. In contrast, diesel combustion proves to be more expensive than alternative options and should therefore at least be questioned for newly built cruise ships of the analyzed size. From a purely economic perspective, gas combustion engines are the most suitable power systems for this specific case study.

While the SOFC system is vastly larger than the conventional ICEs, its size is no counterevidence for usability. Rather, the assessments' level of detail should be increased to a holistic investigation, that considers peripheral equipment, installation flexibility, and the need for extra crew members. Even without further research, the SOFC volume would not bury the environmentally friendly technology in our case study.

As for the environmental aspects, fuel consumption is by far the largest emission source for every system combination. Here, the SOFC technology stands out with high efficiency and the absence of byproducts such as methane and particulate matter. For the investigated ship power class, $CO_2$-equivalent emissions from system production are close to negligible compared to the operational emissions and therefore do not increase the footprint of the SOFC powered system in a meaningful way. Fuel cell technology also reduces the emissions with negative local environmental effects to practically zero. Including the social valuation of greenhouse gases as well as $SO_x$, $NO_x$, and CO, SOFCs come out as the least expensive configuration in this case study.

The compensation of natural gas with a synthetic fuel and the SOFC technology trends until 2050 were also investigated. Smaller aggregate investment costs, reduced degradation and a slightly increased SOFC efficiency lead to a less expensive configuration then the optimally designed gas combustion engine. Further, the social environmental costs of the 2050 SOFC system are only 16% of those for a future ICE solution.

**Declaration of competing interest**

The authors declare that they have no known competing financial interests or personal relationships that could have appeared to influence the work reported in this paper.

**Acknowledgments**

The authors gratefully acknowledge the financial support by the Federal Ministry of Transport and Digital Infrastructure, Germany

(BMVI, funding code 03B10605H) and the coordination of the ‘‘MultiSchIBZ’’ project by the National Organisation Hydrogen and Fuel Cell Technology (NOW GmbH), Germany.

## References


[1] I.M. Organization, Adoption of the initial imo strategy on reduction of ghg emissions from ships and existing imo activity related to reducing ghg emissions in the shipping sector, UNFCCC Talanoa Dialogue (2018).
[2] International Maritime Organization, Fourth greenhouse gas study 2020, 2020.
[3] E. Tzannatos, Ship emissions and their externalities for Greece, Atmos. Environ. (2010).
[4] L. van Biert, A review of fuel cell systems for maritime applications, J. Power Sources (2016).
[5] K. Leites, et al., Schibz - design of different diesel based fuel cell systems for seagoing vessels and their evaluation, ECS Trans. 42 (2012).
[6] EMSA European Maritime Safety Agency, Study on the use of fuel cells in shipping, DNVGL (2017).
[7] C. Wik, S. Niemi, Low emission engine technologies for future tier 3 legislations - options and case studies, J. Shipp. Trade (2016).
[8] P. Marty, et al., Modelling of energy flows and fuel consumption on board ships: application to a large modern cruise vessel and comparison with sea monitoring data, Int. Mar. Des. Conf. (2012).
[9] S. Alkaner, P. Zhou, A comparative study on life cycle analysis of molten carbon fuel cells and diesel engines for marine application, J. Power Sources (2006).
[10] C. Strazza, et al., Comparative LCA of methanol-fuelled SOFCs as auxiliary power systems on-board ships, Appl. Energy (2010).
[11] F. Baldi, et al., The role of solid oxide fuel cells in future ship energy systems, Energy (2020).
[12] K. Kim, G. Roh, W. Kim, K. Chun, A preliminary study on an alternative ship propulsion system fueled by ammonia: Environmental and economic assessments, J. Mar. Sci. Eng. (2020).
[13] E.K. Dedes, et al., Assessing the potential of hybrid energy technology to reduce exhaust emissions from global shipping, Energy Policy 40 (2012).
[14] S. Ros Chaos, et al., Economies of scale in cruise shipping, Marit. Econ. Logist. (2020).
[15] Open Source Modelica Consortium, Openmodelica homepage, 2020, https://www.openmodelica.org/ (Accessed: 2020-09-01).
[16] L. Kistner, A. Bensmann, R. Hanke-Rauschenbach, Optimal design of power gradient limited solid oxide fuel cell systems with hybrid storage support for ship applications, Energy Convers. Manag. (2021).
[17] P. Fortenbacher, G. Andersson, Battery degradation maps for power system optimization and as a benchmark reference, in: 2017 IEEE Manchester PowerTech, 2017.
[18] McKinsey & Company, What shipowners, refiners, and traders should know about IMO 2020, 2021, https://www.mckinsey.com/industries/oil-and-gas/our-insights/what-shipowners-refiners-and-traders-should-know-about-imo-2020 (Accessed: 2021-03-01).
[19] SEA-LNG, The number of vessels using LNG as a marine fuel is growing rapidly, 2021, https://sea-lng.org/why-lng/global-fleet/ (Accessed: 2021-04-07).
[20] H. Schumacher, Einsatzgebiete der dieselmotoren, Dieselmot.-Manag. Überbl.: Einschl. Abgastechnik (2010).
[21] D. Cooper, T. Gustafsson, Methodology for calculating emissions from ships. 1. Update of emission factors, 2004.
[22] S. Ushakov, et al., Methane slip from gas fuelled ships: a comprehensive summary based on measurement data, J. Mar. Sci. Technol. (2019).
[23] M. Caduff, et al., Power-law relationships for estimating mass, fuel consumption and costs of energy conversion equipments, Environ. Sci. Technol. (2011).
[24] Wártsilá, Business white paper - LNG as a marine fuel boosts profitability while ensuring compliance, 2017.
[25] DNV GL, LNG Fuelled perfect, 2020, https://www.dnvgl.de/publications/lng-fuelled-perfect--48498 (Accessed: 2020-09-01).
[26] M. Whiston, et al., Meeting U.S. solid oxide fuel cell targets, Joule (2019).
[27] M. Gianni, et al., Outlook of future implementation of PEMFC and SOFC onboard cruise ships, E3S Web Conf. 238 (2021).
[28] P. Gualeni, et al., Life cycle performance assessment tool development and application with a focus on maintenance aspects, J. Mar. Sci. Eng. (2019).
[29] R. Napoli, et al., Economics evaluation of a 5 kw SOFC power system for residential use, Int. J. Hydrog. Energy 33 (2008).
[30] M. Santin, A. Traverso, L. Magistri, Liquid fuel utilization in SOFC hybrid systems, Appl. Energy (2009).
[31] Maritime Propulsion, Caterpillar mak 16 m 43 C15200hp, 2021, https://www.maritimepropulsion.com/directory/product/mak-16-m-43-c15200hp-500-110175 (Accessed: 2021-01-01).
[32] I.M. Organization, MARPOL Annex VI regulation 14, Int. Conv. Prev. Pollut. Form Ships (2020).
[33] J.J. Corbett, et al., Emissions tradeoffs among alternative marine fuels: total fuel cycle analysis of residual oil, marine gas oil, and marine diesel oil, J. Air Waste Manag. Assoc. (2008).
[34] O. Schinas, M. Butler, Feasibility and commercial considerations of LNG-fueled ships, Ocean Eng. (2016).
[35] DNV GL, Current price development oil and gas, 2020, https://www.dnvgl.com/maritime/lng/current-price-development-oil-and-gas.html (Accessed: 2020-10-01).
[36] M. Altosole, et al., Simulation and performance comparison between diesel and natural gas engines for marine applications, Proc. Inst. Mech. Eng. M: J. Eng. Marit. Environ. (2017).
[37] J.-P. Jalkanen, et al., Extension of an assessment model of ship traffic exhaust emissions for particulate matter and carbon monoxide, Atmos. Chem. Phys. (2012).
[38] statista, Average monthly price of very low sulfur fuel oil (VLSFO) between january and march 2020, 2021, https://www.statista.com/statistics/1109263/monthly-vlsfo-bunker-price-worldwide/ (Accessed: 2021-01-08).
[39] D. Stenersen, et al., D5-6 LNG supply chain feasibility study - overall report, 2008.
[40] K. Sørheim, et al., Characterization of Low Sulfur Fuel Oils (LSFO): A new generation of marine fuel oils, 0000.
[41] International Gas Union, Natural-gas-conversion-guide, 2012, http://members.igu.org/old/IGU%20Events/wgc/wgc-2012/wgc-2012-proceedings/publications/igu-publications (Accessed: 2021-03-01).
[42] R. Edwards, et al., Well-to-Tank Report Version 4a: well-to-wheels analysis of future automotive fuels and powertrains in the european context, 0000.
[43] G. Wu, et al., Emission characteristics for waste cooking oil biodiesel blend in a marine diesel propulsion engine, Polish J. Environ. Stud. (2019).
[44] United States Environmental Protection Agency, Understanding global warming potentials, 2021, https://www.epa.gov/ghgemissions/understanding-global-warming-potentials (Accessed: 2021-03-15).
[45] A. Primas, Maintenance, solid oxide fuel cell 125kw electrical, future - CH, ecoinvent database 3.6, 2007.
[46] A. Avadi, et al., Marine engine construction - GLO, ecoinvent database 3.6, 2014.
[47] A. Primas, Fuel cell production, solid oxide, 125kw electrical, future - CH, ecoinvent database 3.6, 2007.
[48] D. Notter, et al., Battery production, li-ion, rechargeable, prismatic - GLO, ecoinvent database 3.6, 2009.
[49] Thinkstep, Life Cycle GHG Emission Study on the Use of LNG as Marine Fuel: Final Report, 0000.
[50] D. Lack, et al., Particulate emissions from commercial shipping: Chemical, physical, and optical properties, J. Geophys. Res. (2009).
[51] M. Anderson, et al., Particle- and gaseous emissions from an LNG powered ship, Environ. Sci. Technol. (2015).
[52] R. Wurster, et al., LNG als alternativkraftstoff fúr den antrieb von schiffen und schweren nutzfahrzeugen: Kurzstudie im rahmen des auftrags des bundesministeriums fúr verkehr und digitale infrastruktur (BMVI), 2014.
[53] A. Petzold, et al., Experimental studies on particle emissions from cruising ship, their characteristic properties, transformation and atmospheric lifetime in the marine boundary layer, Atmos. Chem. Phys. Discuss. (2007).
[54] World Shipping Council, EU ETS Discussion Paper, 2020.
[55] R. Tol, Targets for global climate policy: An overview, J. Econ. Dyn. Control (2013).
[56] J. van den Bergh, W. Botzen, Monetary valuation of the social cost of CO 2 emissions: A critical survey, Ecol. Econ. (2015).
[57] T.C. Bond, H. Sun, Can reducing black carbon emissions counteract global warming?, Environ. Sci. Technol. (2005).
[58] IPCC, Climate change 2013: The physical science basis: Contribution of working group I to the fifth assessment report of the intergovernmental panel on climate change, 2013.
[59] S. Song, Ship emissions inventory, social cost and eco-efficiency in shanghai yangshan port, Atmos. Environ. (2014).
[60] Ember, Daily EU ETS carbon market price, 2020, https://ember-climate.org/data/carbon-price-viewer/ (Accessed: 2020-11-01).
[61] A. Akimoto, H. Narita, Distribution of SO2, NOx and CO2 emissions from fuel combustion and industrial activities in Asia with 1x1 resolution, Atmos. Environ. 28 (1994).
[62] P. Amoatey, et al., Emissions and exposure assessments of SOX, NOX, PM10/2.5 and trace metals from oil industries: A review study (2000–2018), Process Saf. Environ. Prot. (2019).
[63] R. Verbeek, et al., Environmental and Economic aspects of using LNG as a fuel for shipping in the Netherlands, TNO Report, 2011.
[64] I.-M. Hassellóv, et al., Shipping contributes to ocean acidification, Geophys. Res. Lett. (2013).
[65] D. Mauzerall, et al., NO Emissions from large point sources: variability in ozone production, resulting health damages and economic costs, Atmos. Environ. (2005).
[66] T.-M. Chen, et al., Outdoor air pollution: Nitrogen dioxide, sulfur dioxide, and carbon monoxide health effects, Amer. J. Med. Sci. (2007).
[67] M. Maibach, et al., Handbook on estimation of external cost in the transport sector: Internalisation measures and policies for all external cost of transport (IMPACT), 2008.

[68] A. Miola, et al., Designing a climate change policy for the international maritime transport sector: Market-based measures and technological options for global and regional policy actions, Energy Policy (2011).
[69] K. Birnbaum, et al., Solid oxide fuel cells, sustainability aspects, Fuel Cells (2013).
[70] J. Guilera, et al., Economic viability of SNG production from power and CO2, Energy Convers. Manag. (2018).
[71] J. Gorre, et al., Production costs for synthetic methane in 2030 and 2050 of an optimized power-to-gas plant with intermediate hydrogen storage, Appl. Energy (2019).
[72] A. Dominguez-Ramos, et al., The carbon footprint of power-to-synthetic natural gas by photovoltaicsolar powered electrochemical reduction of CO2, Sustain. Prod. Consum. (2018).
[73] M. Pehl, et al., Understanding future emissions from low-carbon power systems by integration of life-cycle assessment and integrated energy modelling, Nat. Energy (2017).